Direct, indirect, and self-trapped excitons in $Cs_2AgBiBr_6$

Mehmet Baskurt,[1] Paul Erhart,[1] and Julia Wiktor[1,*]

[1] *Chalmers University of Technology, Department of Physics, 41296 Gothenburg, Sweden*

$Cs_2AgBiBr_6$ is a representative halide double perovskite which exhibits promising photovoltaic and light-emitting properties, making it a candidate for next-generation solar cells and LED technologies. Here, we study various possible excited states of this material to understand its absorption and emission properties. We use Time-Dependent Density Functional Theory (TD-DFT) coupled with non-empirical hybrid functionals, specifically PBE0(α) and dielectric-dependent hybrids (DDH) to explore direct, indirect, and self-trapped excitons in this material. Based on comparison with experiment, we show that these methods can give excellent prediction of the absorption spectrum and that the fundamental band gap has been underestimated in previous computational studies. We connect the experimental photoluminescence signals at 1.9-2.0 eV to the emission from self-trapped excitons and electron polarons. Finally, we reveal a complex landscape with energetically competing direct, indirect, and self-trapped excitons in the material.

Halide perovskites (HPs), materials with the general ABX_3 formula, have attracted significant interest for their advanced optoelectronic applications, including solar panels and lighting. A subclass within the HP family, halide double perovskites, replaces the single B metal cation with a combination of two different elements, yielding the $A_2BB'X_6$ formula. Also known as elpasolites, these materials hold potential for applications in photovoltaics, X-ray detection, and white light emission. Among halide double perovskites, $Cs_2AgBiBr_6$ stands out as one of the most studied. It has gained interest as a viable alternative to lead-based perovskites due to its high stability, non-toxicity, outstanding optoelectronic properties, and multifunctionality. Additionally, it has emerged as a benchmark case, both for experimental and computational studies.

One of interesting properties of halide double perovskites is that they often exhibit significant light emission. In $Cs_2AgBiBr_6$, a photoluminescence (PL) peak has been measured at 1.9-2.0 eV[1–3]. This emission has been assigned to the indirect band gap [2, 4, 5] or sub-gap states [6] such as color-centers [1, 3]. It is therefore useful to computationally assess the likelihood of different sources of emission. Since the possible interpretations involve both free (in particular indirect) excitons and self-trapping, such comparison requires a method that can model energetics of delocalized and localized excitations on the same footing.

The study of excited states requires methods extending beyond the density functional theory (DFT), such as the Bethe-Salpeter equation (BSE)[7–11]. However, the high computational cost of BSE makes its use impractical in the case of self-trapped excitons (STEs), which in the most commonly used approach require the use of supercells. One notable exception is a study by Ismail *et al.* [12] on the STE in SiO_2. We note that recent developments by Dai *et al.*[13, 14] made it possible to model STEs in unit cells. However, this technique has not been yet widely applied and in the present study we focus on a cubic perovskite phase, which has been shown to be impossible to describe completely using a small symmetric structure [15–17]. Alternatively, recent advancements have paved the way for more computationally efficient alternatives without compromising the accuracy inherent in BSE. Most notably, the combination of time-dependent density functional theory (TD-DFT) with non-empirical hybrid functionals has been shown to achieve the accuracy of BSE at a fraction of the cost [18, 19]. While this method has been so far used for pristine materials and free excitons, its predictive power and relatively high computational efficiency make it a promising method for studying STEs as well. In a recent study by Jin *et al.* [20] it has been shown that STEs can be efficiently studied using the TD-DFT method. At the same time, they showed that the constrained-occupation DFT method, also called ΔSCF, leads to very similar geometries using TD-DFT forces to relax the structure of the STE.

In the present study, we combine TD-DFT with two types of non-empirical hybrid functionals. One is based on the PBE0(α) functional where the fraction of exact exchange α is set to a value which satisfies the generalized Koopmans' condition [21–23]. Another one belongs to the class of dielectric-dependent hybrid functionals (DDH) [24–26], in which the exchange potential follows the inverse of the dielectric function. From these methods, we extract the transitions of the direct and indirect free excitons as well as of the self-trapped exciton in the singlet and triplet state. We show that different excited states can be close in energy and by performing careful convergence studies we obtain the emission energy from the singlet state of the STE close to the experimental PL signal.

Calculations are performed using two simulation cells. Parametrization of the DDH functional and most convergence tests are done using the unit cell of $Cs_2AgBiBr_6$ (spacegroup $Fm\bar{3}m$) using the experimental lattice parameter of 11.27 Å [27]. Calculations for the free excitons and the STE are done in a supercell containing 320 atoms, based on the polymorphous cubic structure

* julia.wiktor@chalmers.se

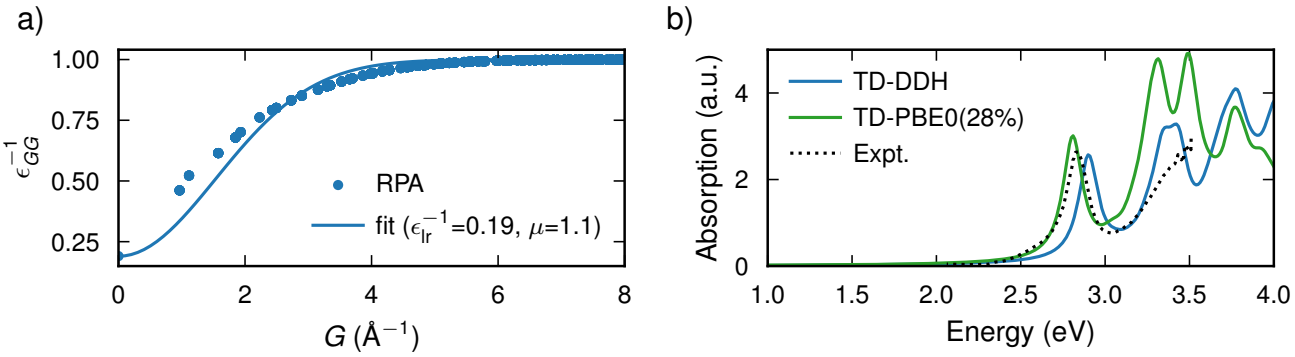

FIG. 1. (a) Inverse dielectric function versus wave vector at the Γ point calculated within the RPA and fitted with Eq. 1. (b) Absorption spectra calculated using TD-DDH and TD-PBE0(28%) compared with the experimental results from Ref. [3].

[16] from Ref. [23], where we used the ΔSCF method for the excited state. In that work, we studied charge localization in $Cs_2AgBiBr_6$ and showed that small electron polarons and STEs are stable in the material, while the localization of small hole polarons is less favorable. We note that these results align well with the later findings by Lafuente-Bartolome *et al.*[28]. From Ref. [23], we adopt the α parameter in PBE0(α) of 0.28, which has been shown to satisfy the Koopmans' condition for the Br vacancy. All simulations presented in the main text include spin-orbit coupling (SOC), while some of the convergence tests shown in the Supporting Information (SI) are done without this contribution. Additional computational details and convergence tests can be found in the SI.

We first calculate the dielectric function ϵ of $Cs_2AgBiBr_6$ within the random-phase approximation (RPA). The calculation is carried out using an energy cutoff of 400 eV and a k-point mesh of 6×6×6. As shown in the SI, these parameters lead to a very well converged dielectric function. The result is given in Fig. 1a in which we also include the fit following:

$$\epsilon^{-1}(G) = 1 - (1 - \epsilon^{-1}_{\rm lr})e^{-G^2/4\mu^2}, \qquad (1)$$

where $\epsilon^{-1}_{\rm lr}$ corresponds to the long-range exchange fraction at $G = 0$, G is the wave vector, and μ is the range-separation parameter. We obtain $\epsilon^{-1}_{\rm lr} = 0.19$ and $\mu = 1.1$.

To verify the validity of our hybrid functionals, we compare the absorption spectra calculated via TD-DFT with experimental results from Ref. [3] (see Fig. 1b). Convergence tests corresponding to the TD-DFT calculations are given in the SI. We observe a very good agreement with the experimental results using both hybrid functional, with TD-PBE0(28%) reproducing the position of the first absorption peak almost exactly and TD-DDH slightly overestimating it, while giving a better agreement for the valley after the first peak. We note that using the nonempirical hybrid functionals we obtain a much better agreement with experimental data than previous G_0W_0 calculations [5, 29], where the position of the first peak was underestimated by about 0.6 eV. This is due to the fact that while non-empirical hybrid functionals have been shown to give high accuracy in describing band gaps of halide perovskites [22, 30], the one-shot G_0W_0 used in Ref. [29] can significantly underestimate that property [15, 31, 32]. We note that while Ref. [5] considered partial self-consistency by updating energies in G and W (the *evGW* scheme), this approach still did not lead to the full increase of the band gap that would reproduce experimental results. In Table I we include the fundamental direct and indirect gaps calculated with the DDH and PBE0(α) methods and compare them with previous computationally reported values (the band structure is given in the SI). First, we note that the two hybrid functionals constructed using different physical considerations lead to almost the same indirect and direct band gaps. Second, we observe that the values present here, about 2.7 and 3.5 eV for the indirect and direct transition, respectively, are much higher than all previous estimates. The highest values from earlier works, 2.1 and 2.7 eV respectively, from partially self-consistent *evGW* calculations, are still lower by 0.6 and 0.8 eV, respectively. Considering the excellent agreement between absorption spectra calculated here and the experiment, we argue that the presented fundamental gaps are more reliable predictions than the previously reported values.

The previous calculations were performed for the perfect cubic structure of $Cs_2AgBiBr_6$. It has been shown that such a symmetric model is not a good representation of the locally and dynamically disordered halide perovskites [15–17]. Therefore, we now turn to the study of the excited states of $Cs_2AgBiBr_6$ based on a more realistic polymorphous model constructed in Ref. [23]. We adopt one polymorphous structure for the pristine $Cs_2AgBiBr_6$ and one for the STE from Ref. [23]. These

structures were generated using the CP2K code [34, 35] and here, for consistency, we further relax the atomic position within VASP. In the following, we focus on the PBE0(28%) functional, as it gives a slightly better agreement with experiment for the lower part of the absorption spectrum. The STE is relaxed within its lowest triplet state and we assume that the atomic positions do not change significantly for the singlet state. We show the isodensities of the localized hole and electron in Figure 2a). We then perform TD-DFT calculation using the two hybrid functionals on top of these geometries. While the relaxation is performed using the Γ point only, for the TD-DFT calculations we use a special grid with four k-points. As shown in the SI, this grid yields lower parts of the absorption spectra that agree well with those from the 2×2×2 grid. The differences in the positions of the two lowest peaks between the two grids are below 0.03 eV. In the pristine material, we observe the lowest transition at 2.45 eV. This transition is dark and corresponds to the lowest indirect exciton. It would not be captured in the unit cell, unless momentum transfers are considered as in Ref. [5]. However, in the supercell used in this study, the X and L points are folded onto the Γ point and are directly accessible by TD-DFT. From the difference between this dark transition and the fundamental band gap in the polymorphous supercell of 2.83 eV we estimate the binding energy of the lowest indirect free exciton to be 0.39 eV. This is slightly lower than the value of 0.48 eV, reported by Palummo *et al.* [5]. The first bright transition, corresponding to the lowest direct free exciton is found at 2.96 eV, while the lowest direct independent-particle transition equals 3.57 eV in the same setup. This implies the binding energy of the direct exciton of 0.61 eV. We note that this value is significantly higher than previously reported ones (0.34 eV in Ref. [5] and 0.17 eV in Ref. [29]), which can be assigned to the higher fundamental band gap of $Cs_2AgBiBr_6$ in the present setup. In their study, Biega *et al.* [29] demonstrated a linear relationship between the exciton binding energy and the size of the direct band gap, which would explain the higher value found here. Additionally, our estimation of the exciton binding energy is based on a polymorphous cell containing local distortions and octahedral tilts, while the previous studies considered unit cells of $Cs_2AgBiBr_6$.

We now analyze the transitions in the TD-DFT calculations for the STE geometry. We note that the calculation corresponds to the excitation from the singlet ground state. However, since absorption and emission are inverse processes, the calculated energy transitions can be expected to be directly comparable to measured photoluminescence spectra. The calculated transitions of the STE are given in Figure 2b). While TD-DFT gives all transitions, we only plot those below 2 eV, as they correspond to the energy range in which photolu-

TABLE I. Fundamental indirect and direct band gaps from the PBE0(α) and DDH functionals compared with previously reported values.

	Indirect gap (eV)	Direct gap (eV)
PBE0(28%)	2.66	3.52
DDH	2.66	3.50
G_0W_0 Ref. [33]	1.83	2.51
G_0W_0 Ref. [29]	1.66	2.41
evGW Ref. [5]	2.1	2.7

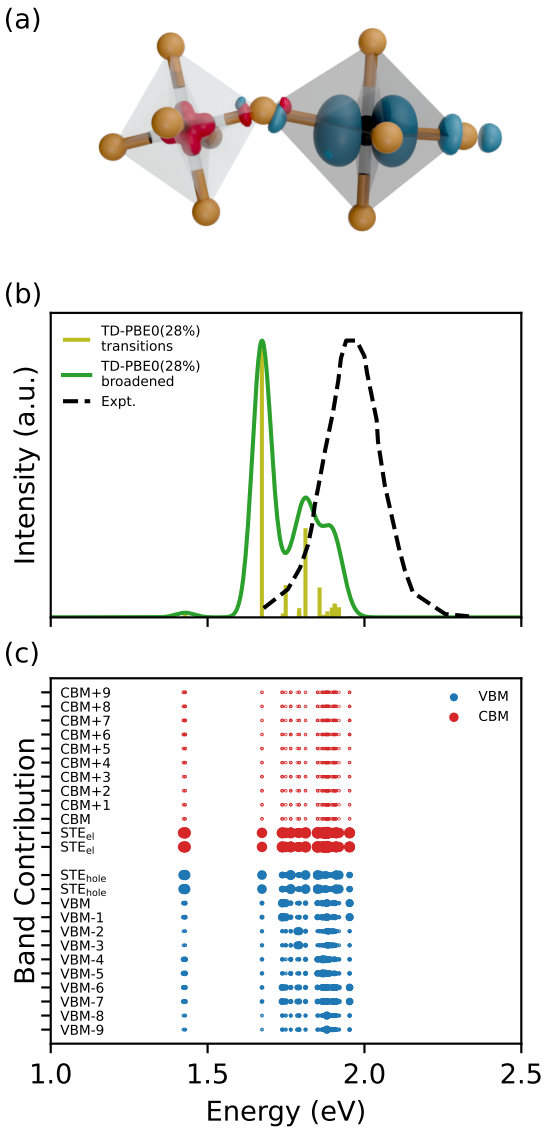

FIG. 2. (a) Isodensities of the hole (in red) and electron (in blue), localized within the $AgBr_6$ and $BiBr_6$ octahedron, respectively. The rest of the structure was removed for clarity. (b) Emission from the STE compared with the experimental PL spectrum from Ref. [3]. The broadened spectrum was generated by convolution with Gaussians with a width of 0.03 eV. All spectra were rescaled to have the same maximum. (c) Band contributions to each of the transitions marked in the upper panel. For each initial (final) state, the contributions of different final (initial) states, as well as all k-points, are added up.

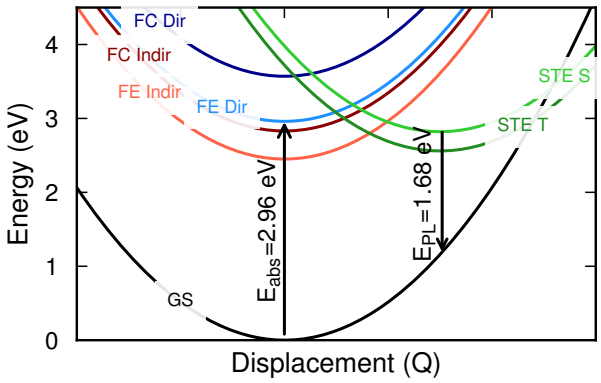

FIG. 3. Configuration coordinate diagram of different electron-hole pairs in $Cs_2AgBiBr_6$, including free carriers (FC), free excitons (FE) and self-trapped excitons (STE). 'Indir' and 'Dir' refer to indirect and direct transitions, and 'S' and 'T' to singlet and triplet states.

minescence is measured. We compare the results with the experimental PL spectrum from Ref. [3]. The measurement was done at 4 K, hence the phonon broadening can be neglected in the comparison. While the simulated spectrum is at lower energies than the experimental one, the difference between the middles of the spectra is only about 0.2 eV, representing fairly good agreement. We also note that the broadness of the experimental peak at low temperatures can be explained by the distribution of transitions which contribute to it. In Figure 2c) we show the band composition of the calculated transitions. The lowest transition at 1.42 eV has a very low intensity and corresponds to a spin-forbidden triplet-singlet transition between the localized electron and hole states from within the STE. Then, at 1.68 eV there is a bright transition from the singlet state of the STE. This implies a separation of 0.26 eV between the lowest triplet and higher singlet states of the STE in $Cs_2AgBiBr_6$. At higher energies, between 1.74–1.95 eV, there is a distribution of transitions which all involve the localized electron state and both localized and delocalized hole states. This range of energies can be used as an estimate of PL stemming from the electron polaron, if the STE dissociates. In this energy range, we do not observe any transitions between the localized hole and delocalized electrons, because the hole in the STE has a more shallow level than the electron and this type of emission would mostly overlap with the absorption onset close to 3 eV.

Using the energy transitions from the TD-DFT calculations, we finally construct the configuration coordinate diagram. It allows us to compare the energies of direct, indirect and self-trapped excitons. The diagram, given in Figure 3 is based on TD-PBE0(28%) calculations in the polymorphous cubic supercell. The diagram reveals a complex landscape of electron-hole excitations in the material and can be used to analyze the dynamics of the excited charges. First, direct free excitons are created. These free excitons can then be trapped, in the form of the singlet STE. This STE can then undergo four processes. One, it can recombine leading to a bright emission that can be measured in photoluminescence. Two, it can lower its energy and turn into a triplet form of STE. Three, it can detrap and become an indirect free exciton, which has an energy very close to that of the triplet STE (within 0.1 eV in the current computational setup). Finally, it could also dissociate leaving behind a localized electron and possibly a delocalized hole [23].

In conclusion, we have studied different types of excitons in $Cs_2AgBiBr_6$ halide double perovskites. We first assessed the performance of two non-empirical hybrid functionals, PBE0(28%) and DDH in the description of the optical properties of the pristine material. We have shown that both of them predict band gaps higher than what was previously reported in the literature and give absorption spectra in very good agreement with experiment. We then used the TD-PBE0(28%) technique to study excitations in the polymorphous cubic supercells corresponding to the ground-state structure and the self-trapped exciton. This allowed us to show that the emission from the STE is in good agreement with experimental PL spectra. Based on a configuration coordinate diagram, we finally revealed a complex landscape of electron-hole pairs in the materials with direct, indirect and self-trapped excitons having comparable energies.

ACKNOWLEDGMENTS

This work was supported by the Swedish Research Council (grant numbers 2019-03993, and 2020-04935), the Swedish Strategic Research Foundation through a Future Research Leader program (FFL21-0129) and the Wallenberg Academy Fellow program. The computations were enabled by resources provided by the National Academic Infrastructure for Supercomputing in Sweden (NAISS) at C3SE, NSC, and PDC partially funded by the Swedish Research Council through grant agreements no. 2022-06725 and no. 2018-05973.

[1] S. Zelewski, J. Urban, A. Surrente, D. K. Maude, A. Kuc, L. Schade, R. Johnson, M. Dollmann, P. Nayak, H. Snaith, P. Radaelli, R. Kudrawiec, R. J. Nicholas, P. Plochocka, and M. Baranowski, J. Mater. Chem. C **7**, 8350 (2019).

[2] L. Schade, A. D. Wright, R. D. Johnson, M. Dollmann, B. Wenger, P. K. Nayak, D. Prabhakaran, L. M. Herz, R. Nicholas, H. J. Snaith, *et al.*, ACS Energy Lett. **4**, 299

(2018).
[3] A. D. Wright, L. R. Buizza, K. J. Savill, G. Longo, H. J. Snaith, M. B. Johnston, and L. M. Herz, J. Phys. Chem. Lett. **12**, 3352 (2021).
[4] A. H. Slavney, T. Hu, A. M. Lindenberg, and H. I. Karunadasa, J. Am. Chem. Soc. **138**, 2138 (2016).
[5] M. Palummo, E. Berrios, D. Varsano, and G. Giorgi, ACS Energy Lett. **5**, 457 (2020).
[6] R. L. Hoye, L. Eyre, F. Wei, F. Brivio, A. Sadhanala, S. Sun, W. Li, K. H. Zhang, J. L. MacManus-Driscoll, P. D. Bristowe, *et al.*, Adv. Mater. Interfaces **5**, 1800464 (2018).
[7] S. Albrecht, L. Reining, R. Del Sole, and G. Onida, Phys. Rev. Lett. **80**, 4510 (1998).
[8] M. Rohlfing and S. G. Louie, Phys. Rev. Lett. **80**, 3320 (1998).
[9] L. X. Benedict, E. L. Shirley, and R. B. Bohn, Phys. Rev. Lett. **80**, 4514 (1998).
[10] G. Onida, L. Reining, and A. Rubio, Rev. Mod. Phys. **74**, 601 (2002).
[11] H.-Y. Sun, L. Xiong, and H. Jiang, Chem. Phys. Rev. **4** (2023).
[12] S. Ismail-Beigi and S. G. Louie, Phys. Rev. Lett. **95**, 156401 (2005).
[13] Z. Dai, C. Lian, J. Lafuente-Bartolome, and F. Giustino, Phys. Rev. Lett. **132**, 036902 (2024).
[14] Z. Dai, C. Lian, J. Lafuente-Bartolome, and F. Giustino, Phys. Rev. B **109**, 045202 (2024).
[15] J. Wiktor, U. Rothlisberger, and A. Pasquarello, J. Phys. Chem. Lett. **8**, 5507 (2017).
[16] X.-G. Zhao, G. M. Dalpian, Z. Wang, and A. Zunger, Phys. Rev. B **101**, 155137 (2020).
[17] J. Wiktor, E. Fransson, D. Kubicki, and P. Erhart, Chem. Mater. **35**, 6737 (2023).
[18] J. Sun, J. Yang, and C. A. Ullrich, Phys. Rev. Res. **2**, 013091 (2020).
[19] A. Tal, P. Liu, G. Kresse, and A. Pasquarello, Phys. Rev. Res. **2**, 032019 (2020).
[20] Y. Jin, M. Rusishvili, M. Govoni, and G. Galli, J. Phys. Chem. Lett. **15**, 3229 (2024).
[21] I. Dabo, A. Ferretti, N. Poilvert, Y. Li, N. Marzari, and M. Cococcioni, Phys. Rev. B **82**, 115121 (2010).
[22] T. Bischoff, J. Wiktor, W. Chen, and A. Pasquarello, Phys. Rev. Mater. **3**, 123802 (2019).
[23] M. Baskurt and J. Wiktor, J. Phys. Chem. C **127**, 23966 (2023).
[24] W. Chen, G. Miceli, G.-M. Rignanese, and A. Pasquarello, Phys. Rev. Mater. **2**, 073803 (2018).
[25] Z.-H. Cui, Y.-C. Wang, M.-Y. Zhang, X. Xu, and H. Jiang, J. Phys. Chem. Lett. **9**, 2338 (2018).
[26] P. Liu, C. Franchini, M. Marsman, and G. Kresse, J. Phys.: Condens. Matter **32**, 015502 (2019).
[27] W. Ning, J. Bao, Y. Puttisong, F. Moro, L. Kobera, S. Shimono, L. Wang, F. Ji, M. Cuartero, S. Kawaguchi, S. Abbrent, H. Ishibashi, R. D. Marco, I. A. Bouianova, G. A. Crespo, Y. Kubota, J. Brus, D. Y. Chung, L. Sun, W. M. Chen, M. G. Kanatzidis, and F. Gao, Sci. Adv. **6**, eabb5381 (2020).
[28] J. Lafuente-Bartolome, C. Lian, and F. Giustino, Proc. Natl. Acad. Sci. U.S.A. **121**, e2318151121 (2024).
[29] R.-I. Biega, M. R. Filip, L. Leppert, and J. B. Neaton, J. Phys. Chem. Lett. **12**, 2057 (2021).
[30] H. Wang, A. Tal, T. Bischoff, P. Gono, and A. Pasquarello, npj Comput. Mater. **8**, 237 (2022).
[31] M. R. Filip and F. Giustino, Phys. Rev. B **90**, 245145 (2014).
[32] L. Leppert, T. Rangel, and J. B. Neaton, Phys. Rev. Mater. **3**, 103803 (2019).
[33] M. R. Filip, S. Hillman, A. A. Haghighirad, H. J. Snaith, and F. Giustino, J. Phys. Chem. Lett. **7**, 2579 (2016).
[34] J. VandeVondele, M. Krack, F. Mohamed, M. Parrinello, T. Chassaing, and J. Hutter, Comput. Phys. Commun. **167**, 103 (2005).
[35] T. D. Kühne, M. Iannuzzi, M. Del Ben, V. V. Rybkin, P. Seewald, F. Stein, T. Laino, R. Z. Khaliullin, O. Schütt, F. Schiffmann, D. Golze, J. Wilhelm, S. Chulkov, M. H. Bani-Hashemian, V. Weber, U. Borštnik, M. Taillefumier, A. S. Jakobovits, A. Lazzaro, H. Pabst, T. Müller, R. Schade, M. Guidon, S. Andermatt, N. Holmberg, G. K. Schenter, A. Hehn, A. Bussy, F. Belleflamme, G. Tabacchi, A. Glöß, M. Lass, I. Bethune, C. J. Mundy, C. Plessl, M. Watkins, J. VandeVondele, M. Krack, and J. Hutter, J. Chem. Phys. **152**, 194103 (2020).

Supporting Information:

Direct, indirect, and self-trapped excitons in $Cs_2AgBiBr_6$

Mehmet Baskurt[1], Paul Erhart[1], and Julia Wiktor[1,*]

[1] *Department of Physics, Chalmers University of Technology, SE-41296, Gothenburg, Sweden*
[*] *julia.wiktor@chalmers.se*

1 Computational details

All calculations in the main text are done within the Projector Augmented-Wave (PAW) method, as implemented in the VASP software package.[1,2] The atomic position in the unit cell were first relaxed within the SCAN+rVV10 functional[3], which has been shown to give very good predictions of structural properties of halide perovskites.[4] As the valence states, we consider $5s^2 5p^6 6s^1$ for Cs, $4d^{10} 5s^1$ for Ag, $6s^2 6p^3$ for Bi, and $4s^2 4p^5$ for Br. We note that in a recent study, Wang *et al.*[5] showed that including semicore states has an important effect on the band gaps of $Cs_2AgBiBr_6$ calculated combining norm-conserving pseudofunctionals and hybrid functionals. We verified that, when using the PAW method, including one additional shell in the valence states of Ag, Bi, and Br increases the band gap by only 0.08 eV and 0.05 eV with the DDH and PBE0(28%) functionals, respectively. Therefore, we conclude that the issue observed by Wang *et al.* is specific to norm-conserving pseudopotentials.

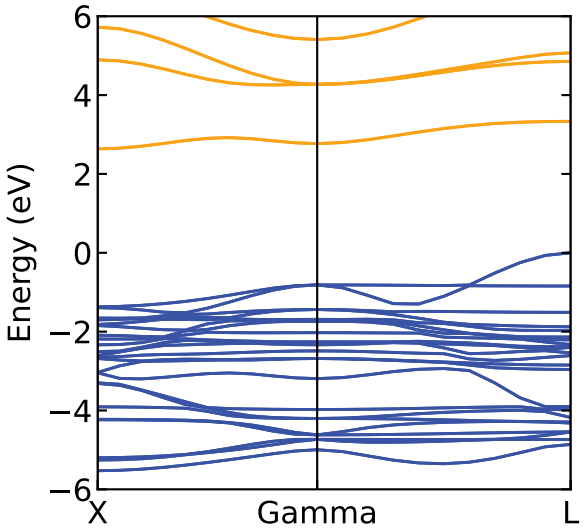

Figure 1: Band structure of $Cs_2AgBiBr_6$ calculated within the PBE0(28%) functional.

We calculate the frequency-dependent dielectric function in the unit cell within the Random Phase Approximation (RPA). We verify the convergence with the cutoff energy and the k-point grid and find that the dielectric function is well converged with the grid of 4×4×4 and cutoff of 400 eV.

Next, we test the convergence of the absorption spectra calculated within the TD-PBE0(28%) method in the unit cell. We find that the lower part of the spectrum is well converged using the cutoff of 200 eV, the k-point grid of 6×6×6 and considering 10 occupied and 10 unoccupied bands in the Casida equation. We note that we apply here the Tamm-Dancoff approximation.

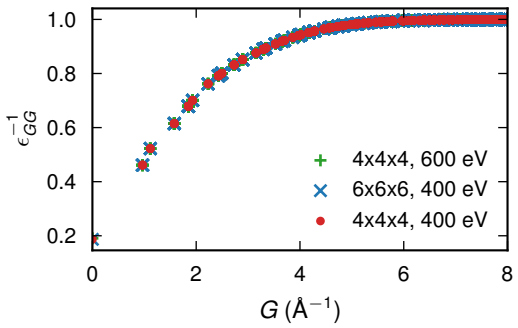

Figure 2: Convergence of the dielectric function with respect to the k-point grid and cutoff energy.

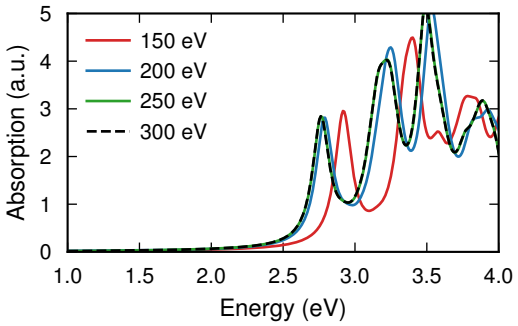

Figure 3: Convergence of the absorption spectrum with respect to the cutoff energy.

We perform separate convergence tests for the supercell calculations. While the cutoff energy remains the same, we verify the convergence of the absorption spectra with respect to the k-point mesh and the number of occupied and unoccupied states in the Casida equation. To speed up the convergence with the number of k-points, we use a special grid with 4 points at (0,0,0), (0,0.5,0.5), (0.5,0,0.5), and (0.5,0.5,0). This grid gives absorption spectra in good agreement with the 2×2×2 grid and is used in the main text. We observe that increasing the density of k-points shifts the peaks in the absorption spectra to slightly higher energies. Conversely, increasing the number of states considered in the Casida equation shifts the peaks to lower energies. Therefore, we anticipate a significant cancellation of errors between these two convergence parameters.

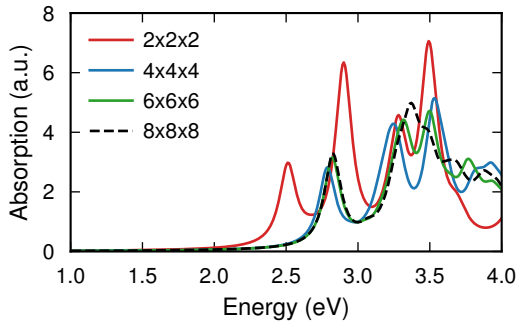

Figure 4: Convergence of the absorption spectrum with respect to the k-point grid.

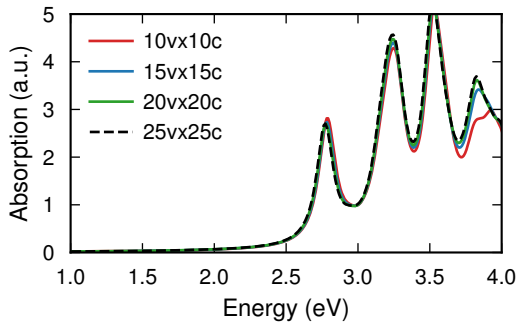

Figure 5: Convergence of the absorption spectrum with respect to numbers of occupied and unoccupied bands included in the Casida equation.

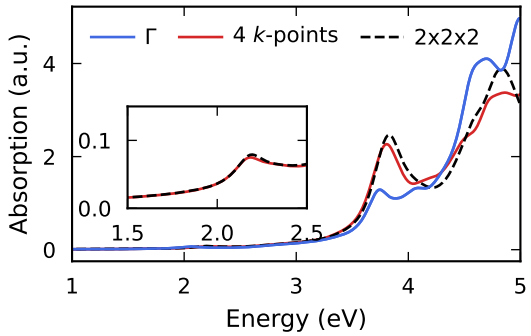

Figure 6: Convergence of the absorption spectrum calculated on the ground state in the geometry of the STE with respect to the number of k-points. The convergence tests was carried out without SOC.

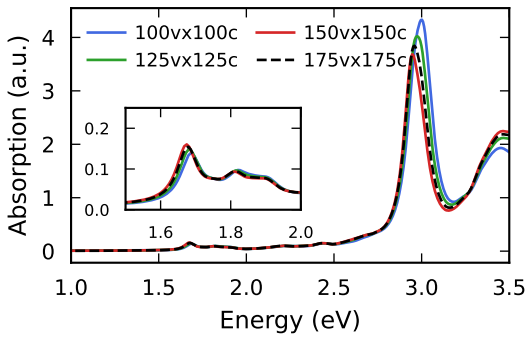

Figure 7: Convergence of the absorption spectrum calculated on the ground state in the geometry of the STE with respect to the number of occupied and unoccupied bands included in the Casida equation.

References

[1] Georg Kresse and Jürgen Hafner. Ab initio molecular dynamics for liquid metals. *Phys. Rev. B*, 47(1):558, 1993.

[2] Georg Kresse and Jürgen Furthmüller. Efficient iterative schemes for ab initio total-energy calculations using a plane-wave basis set. *Phys. Rev. B*, 54(16):11169, 1996.

[3] Haowei Peng, Zeng-Hui Yang, John P Perdew, and Jianwei Sun. Versatile van der waals density functional based on a meta-generalized gradient approximation. *Phys. Rev. X*, 6(4):041005, 2016.

[4] Julia Wiktor, Erik Fransson, Dominik Kubicki, and Paul Erhart. Quantifying dynamic tilting in halide perovskites: Chemical trends and local correlations. *Chem. Mater.*, 35(17):6737–6744, 2023.

[5] Haiyuan Wang, Runhai Ouyang, Wei Chen, and Alfredo Pasquarello. High-quality data enabling universality of band gap descriptor and discovery of photovoltaic perovskites. *J. Am. Chem. Soc.*, 2024.